

Exploiting barrier distributions to investigate breakup effects in the fusion of ${}^9\text{Be} + {}^{208}\text{Pb}$

M DASGUPTA¹, D J HINDE¹, R D BUTT¹, A C BERRIMAN¹, C R MORTON¹,
J O NEWTON¹ and K HAGINO²

¹Department of Nuclear Physics, Research School of Physical Sciences and Engineering, Australian National University, Canberra, ACT 0200, Australia

²Institute for Nuclear Theory, Department of Physics, University of Washington, Seattle, WA98915, USA

Abstract. The availability of precisely measured fusion excitation functions have allowed the determination of experimental fusion barrier distributions. This concept is utilised in ${}^9\text{Be} + {}^{208}\text{Pb}$ reaction, to reliably predict the expected complete fusion cross-sections. However, the measured cross-sections are found to be only 68% of those predicted. The large cross-sections observed for incomplete fusion products support the interpretation that this suppression of fusion is caused by ${}^9\text{Be}$ breaking up into charged fragments before reaching the fusion barrier.

Keywords. Fusion; barrier distribution; breakup; incomplete fusion.

PACS No. 25.70.Jj

1. Introduction

It is now well accepted that fusion near the Coulomb barrier is strongly affected [1,2] by intrinsic degrees of freedom of the interacting nuclei, whose coupling with the relative motion effectively causes a splitting in energy of the single, uncoupled fusion barrier. This gives rise to a distribution of barrier heights [3], some higher and some lower in energy than the uncoupled barrier. The experimental effort towards obtaining precisely measured [4–8] fusion cross-sections has been extremely successful, with one of the main outcomes being the ability to extract an *experimental* fusion barrier distribution [9]. This, combined with improved theoretical models has led to a better, in some cases quantitative, understanding of the effects induced by target and projectile structure, as discussed by Rowley [10], Stefanini [11] and others [12] during this workshop.

We are now at a stage where we can start to exploit our knowledge of the near-barrier fusion process in order to explain properties of the compound nucleus and its decay. For example, this has helped in understanding the strong enhancement of the superdeformed band population in ${}^{135}\text{Nd}$ [13]. The renewed confidence in calculations of sub-barrier fusion angular momentum distributions has led to explanations [14] for the anomalously large fission fragment anisotropies observed in reactions with actinide nuclei in terms of the dynamics of the fusion process, rather than in terms of flaws in fusion models. Knowledge

of the fusion process with stable beams is also the first step towards understanding fusion with unstable nuclei and it is this aspect that will be discussed in this paper.

The advent of radioactive beam facilities has enabled the study of unstable neutron-rich nuclei which have very weakly bound neutrons and exhibit characteristic features such as a neutron halo [15] extending to large radii, and a low energy threshold for breakup. The extended nuclear matter distribution is expected to lead [16] to a lower fusion barrier, and thus to an enhancement in fusion cross-sections [17] compared to those for tightly bound nuclei. The effect of couplings to channels which act as doorways to breakup is, however, controversial [18–21]. Any coupling will enhance the sub-barrier cross-sections, whereas breakup may result in capture of only a part of the projectile, thus suppressing complete fusion. Model predictions [18–20], however, differ in the relative magnitudes of enhancement and suppression. To investigate these aspects, fusion excitation functions for ${}^9,{}^{11}\text{Be} + {}^{238}\text{U}$ [22] and ${}^9,{}^{10,}{}^{11}\text{Be} + {}^{209}\text{Bi}$ [23] were measured at energies around the barrier. The reactions with the stable ${}^9\text{Be}$ were included for comparison. The fusion cross-sections for ${}^{10,}{}^{11}\text{Be} + {}^{209}\text{Bi}$ at energies near and below the barrier were found to be similar to those for ${}^9\text{Be}$, while above the barrier the ${}^9\text{Be}$ induced reaction gave the lowest fusion yield. It is not obvious whether this is due to differing enhancement or suppression for the stable and unstable projectiles.

To investigate the effect on fusion of couplings specific to unstable neutron-rich nuclei, it is necessary to reliably predict the cross-sections expected in their absence. Thus, in the above cases, definitive conclusions are difficult unless fusion with ${}^9\text{Be}$ is well understood. This requires knowledge of the energy of the average fusion barrier, and information on the couplings. Both these can be obtained from the distribution of fusion barriers extracted from a precisely measured fusion excitation function. The shape of the experimental barrier distribution is indicative of the couplings present and its centroid gives the average barrier position. Precise fusion excitation function measurements [24] for the reaction ${}^9\text{Be} + {}^{208}\text{Pb}$, with the aim of extracting the barrier distribution, were therefore made at the Australian National University. The experimental details are described in the next section. Section 3 discusses the identification of the products of complete fusion, followed by §4 where the result of the experimental determination of average barrier energy, along with the comparison with coupled channels calculations are presented. Section 5 presents the results of the incomplete fusion measurements, followed by a summary in §6.

2. The experiment

The experiments were performed with pulsed ${}^9\text{Be}$ beams (1 ns on, 1 μs off) in the energy range 35.0–51.0 MeV in 1 MeV steps, from the 14UD tandem accelerator at the Australian National University. Targets were of enriched ${}^{208}\text{PbS}$, 340–400 $\mu\text{g}/\text{cm}^2$ in thickness, evaporated onto 15 $\mu\text{g}/\text{cm}^2$ C foils. Two monitor detectors, placed above and below the beam axis, measured the elastically scattered beam particles for normalization purposes. Recoiling heavy reaction products were stopped in aluminium catcher foils of thickness 360 $\mu\text{g}/\text{cm}^2$, placed immediately behind the target. The cross-sections for the reaction products or the evaporation residues were determined by measuring the α -particles emitted during their subsequent decay. The products were identified by their distinctive α -energies and half-lives (270 ns to 138 days). Alpha particles from short-lived activity (half-life $T_{1/2} \leq 26$ s) were measured *in situ* between the beam bursts, using an annular silicon

surface barrier detector placed at a mean angle of 174° to the beam direction. These were measured at all beam energies using the same target. This eliminated uncertainties in the beam energy difference between data points which would result from the use of different targets. Fusion evaporation residues at energies higher than 47 MeV are long-lived ($T_{1/2} \geq 24$ min). Their cross-sections were determined by using an un-irradiated target and catcher at each energy. Alpha particles from these products were measured using a silicon surface barrier detector situated below the annular counter, such that the target and catcher could be placed at a close geometry to the detector after the irradiation. The relative solid angles of the two detectors were determined using the $T_{1/2} = 24$ min ${}^{212}\text{Rn}$ activity.

Fission following fusion was measured during the irradiations using two large area position sensitive multi-wire proportional counters (MWPCs), centred at 45° and -135° to the beam direction. Absolute cross-sections for evaporation residues and fission were determined by performing calibrations at sub-barrier energies in which elastically-scattered projectiles were detected in the two monitor detectors, the annular detector and the backward-angle MWPC.

3. Identification of the products of complete fusion

The compound nucleus ${}^{217}\text{Rn}$ formed following complete fusion of ${}^9\text{Be}$ with ${}^{208}\text{Pb}$ cools mainly by neutron evaporation. The measured cross-sections for $2n$, $3n$, $4n$ and $5n$ evaporation residues are shown in figure 1a. No proton evaporation residues were observed. In addition to the α -particles from the decay of Rn nuclei, α -particles from the decay of ${}^{210,211}\text{Po}$ and ${}^{212}\text{Po}$ nuclei were also observed as shown by hollow points and filled diamonds respectively in figure 1b. Po nuclei are formed as daughters of the Rn nuclei following their α -decay. However, the observed Po yields are much greater than expected from the Rn yields. The filled points show the ${}^{210,211,212}\text{Po}$ yields obtained after subtraction of the component resulting from the decay of the Po nuclei, formed as daughters of the Rn nuclei. The non-zero values of the Po yields are a clear indication that there is also a direct population mechanism. In principle the Po nuclei could originate from complete fusion followed by αxn evaporation. However the shapes of the excitation functions for these nuclei are distinctly different from those in figure 1a, and are not typical of fusion-evaporation.

To investigate the origin of the Po yield, the same compound nucleus ${}^{217}\text{Rn}$ was formed at similar excitation energies in the reaction ${}^{13}\text{C} + {}^{204}\text{Hg}$. The ${}^{211,212}\text{Po}$ α -decays, to which the measurement was most sensitive, had cross-sections of <5 mb, compared with a total of ~ 160 mb for the ${}^9\text{Be} + {}^{208}\text{Pb}$ reaction. Furthermore, the fusion cross-sections determined from the sum of the xn evaporation and fission cross-sections agreed with the predictions of a coupled channels calculation and the Bass model [25], indicating that the xn evaporation yield essentially exhausts the total evaporation residue cross-section. Thus, the direct Po production observed in the ${}^9\text{Be}$ reaction cannot be due to complete fusion. It is attributed to incomplete fusion, and will be discussed in §5. The observed fission cross-sections were attributed to complete fusion of ${}^9\text{Be} + {}^{208}\text{Pb}$, since fission following incomplete fusion should be negligible due to the lower angular momentum and excitation energy brought in, and the higher fission barriers of the resulting compound nuclei.

Thus, the cross-section for complete fusion, defined as the capture of all the charge of the ${}^9\text{Be}$ projectile, was obtained by summing the Rn xn evaporation residue cross-sections and the fission cross-section at each energy.

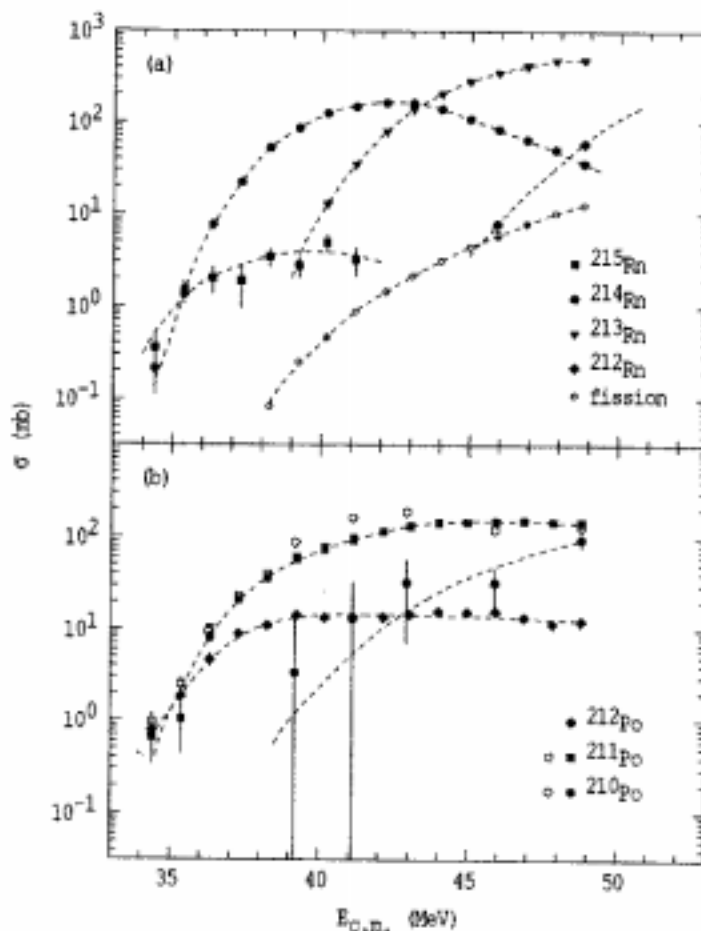


Figure 1. (a) The measured cross-sections for fission and the production of Rn isotopes. (b) The total (hollow points) and the direct (solid points) production of the Po isotopes as indicated. The dashed lines guide the eye.

4. Determination of the barrier height and comparison with calculations

The excitation function for complete fusion and the experimental barrier distribution $d^2(E\sigma_{\text{fus}})/dE^2$ are shown by the filled circles in figure 2a and 2b, respectively. The barrier distribution has been evaluated using a point difference formula [6] with a c.m. energy step of 1.92 MeV. The average barrier position obtained from the experimental barrier distribution is 38.3 ± 0.6 MeV. To predict the fusion cross-sections expected from the measured barrier distribution, realistic coupled channels calculations [26] were performed using a Woods–Saxon form for the nuclear potential chosen such that the average barrier energy of these calculations matched that measured. Couplings to the $5/2^-$ and $7/2^-$ states

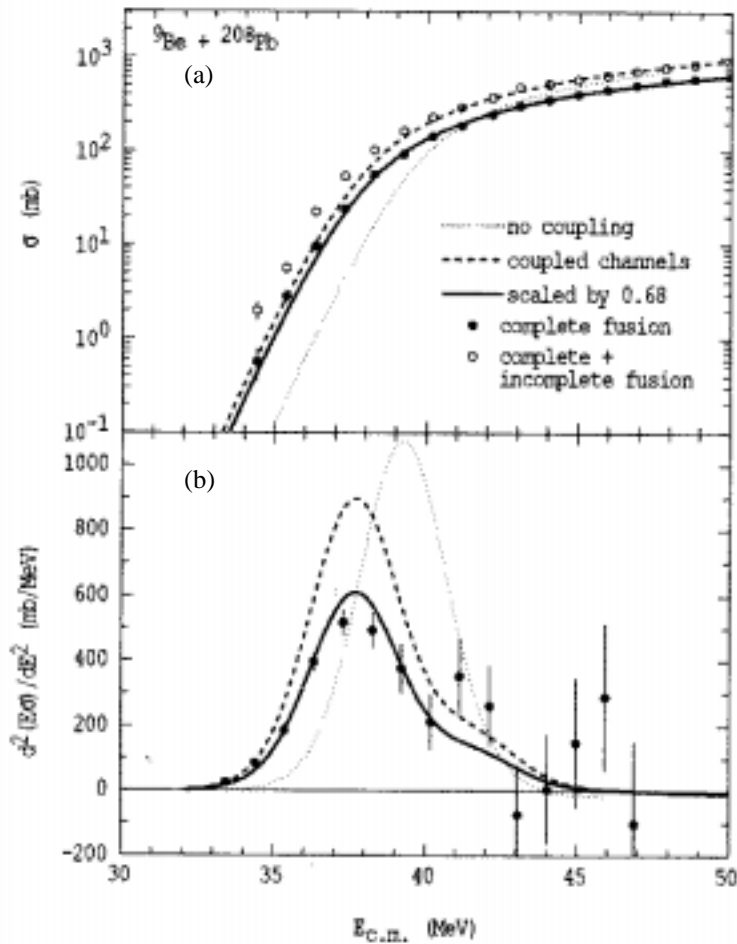


Figure 2. (a) The excitation function for complete fusion (filled circles) and (b) the barrier distribution for the reaction ${}^9\text{Be} + {}^{208}\text{Pb}$. The dotted line shows the calculation assuming a single barrier. The dashed line is the result of a coupled channels calculation (see text) which ignores breakup effects. The full line is the same calculation scaled by 0.68. The sum of measured complete and incomplete fusion cross-sections is given by the hollow circles.

of the $K^\pi = 3/2^-$ ground-state rotational band [27] in ${}^9\text{Be}$, and to the $3^-, 5^-$ and the double octupole-phonon [28,29] states in ${}^{208}\text{Pb}$, were included. Coupling strengths were obtained from the experimental ground state quadrupole moment [27] of ${}^9\text{Be}$, and experimental deformation lengths [30] for one-phonon states in ${}^{208}\text{Pb}$. Couplings to the double octupole-phonon states in ${}^{208}\text{Pb}$ were calculated in the harmonic limit.

The results of these calculations are shown in figure 2a and 2b by the dashed lines. They reproduce satisfactorily the asymmetric shape of the measured barrier distribution. The area under the calculated distribution is a measure of the geometrical cross-section πR^2 ,

where R is the fusion barrier radius. The measured distribution shows a much smaller area than the calculation, despite the barrier energies being in agreement. This disagreement is necessarily reflected in the cross-sections as well, where the calculated values are considerably larger than those measured. This is in contrast to fusion with tightly bound projectiles [4–8], such as ^{16}O and ^{19}F , where calculations which correctly reproduce the average barrier position and the shape of the barrier distribution, and hence has the right potential parameters and couplings, give an extremely good fit to the cross-sections. The disagreement for $^9\text{Be} + ^{208}\text{Pb}$, even though the barrier energies are correctly reproduced, suggests the presence of a mechanism hindering fusion. Agreement can be achieved if the calculated fusion cross-sections are scaled by 0.68, resulting in the full lines in figure 2a and 2b. This scaling factor will be model dependent at the lowest energies, as the calculations are sensitive to the types of coupling and their strength. However, at energies around and above the average barrier, the scaling factor is more robust, since changes in the couplings or potential shape within the constraints of the measured barrier distribution, does affect the calculations significantly. The suppression factor of 0.68 has an uncertainty of ± 0.07 arising from the uncertainty in the mean barrier energy.

5. Incomplete fusion

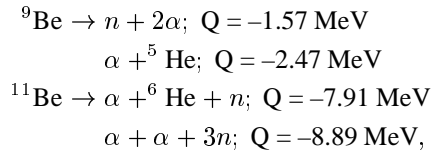
The suppression of complete fusion discussed above, may be correlated with the large yields of $^{210,211,212}\text{Po}$ which, as mentioned in §3, are not the products of complete fusion. These can be formed if ^9Be breaks up into $^4,5\text{He}$ or two α particles and a neutron, and one of the charged fragments is captured by the ^{208}Pb . If all the fragments are captured then this process cannot be distinguished experimentally from fusion without breakup, and is included in the complete fusion yield. Incomplete fusion products following the breakup of ^9Be giving $^{6,7,8}\text{Li}$ were not observed; they are unfavoured due to large negative Q values. The large cross-sections for incomplete fusion, approximately half of those for complete fusion, demonstrate that ^9Be has a substantial probability of breaking up into charged fragments. The sum of the complete and incomplete fusion cross-sections is indicated by the hollow circles in figure 2a. It is interesting to note that they match the predictions of the un-scaled coupled channels fusion calculation, suggesting a direct relationship between the flux lost from fusion and the incomplete fusion yields. However, such a simple direct comparison is not strictly possible, since the cross-sections for incomplete fusion may include contributions from higher partial waves which may not have led to complete fusion.

The suppression of fusion observed in this experiment can be attributed to a reduction of flux at the fusion barrier radius due to breakup of the ^9Be projectiles. It would be interesting to investigate whether the breakup is dominated by the long range Coulomb or the short range nuclear interaction. Comparison of the present results with those existing for lighter targets [31–33] may give additional insights.

6. Discussion and summary

In studies of breakup effects for neutron-rich unstable nuclei, attention has been on the neutron separation energy [34], which for ^{11}Be is 0.50 MeV, compared with 1.67 MeV for ^9Be . This led to the expectation that breakup effects in ^{11}Be induced reactions would affect

(suppress or enhance depending on the theoretical approach) fusion more strongly compared with those induced by ${}^9\text{Be}$. However, the experimental data could not be explained on this basis. The present experiment demonstrates that breakup into charged fragments affects fusion very significantly. The two most favourable charged fragmentation channels for ${}^9,{}^{11}\text{Be}$ are :



making ${}^9\text{Be}$ more unstable in this regard than ${}^{11}\text{Be}$. Reactions with ${}^9\text{Be}$ therefore offer an excellent opportunity to study breakup and its effect on fusion, but they should not be taken as a stable standard against which to judge the breakup effects of unstable nuclei.

In summary, precise complete and incomplete fusion cross-sections have been measured [24] for ${}^9\text{Be} + {}^{208}\text{Pb}$ near the Coulomb barrier. The barrier distribution for complete fusion shows conclusively that complete fusion of ${}^9\text{Be}$ is suppressed compared with the fusion of more tightly bound nuclei. The calculated fusion cross-sections need to be scaled by a factor 0.68 ± 0.07 in order to obtain a consistent representation of the measured fusion excitation function and barrier distribution. The loss of flux at the fusion barrier implied by this result can be related to the observed large cross-sections for Po nuclei, demonstrating that ${}^9\text{Be}$ has a large probability of breaking up into two helium nuclei, which suppresses the complete fusion yield. These measurements, in conjunction with breakup cross-sections and elastic scattering data, should encourage a complete theoretical description of fusion and breakup.

References

- [1] M Beckerman, *Rep. Prog. Phys.* **51**, 1047 (1988) and references therein
- [2] M Dasgupta *et al*, *Annu. Rev. Nucl. Part. Sci.* (in Press)
- [3] C H Dasso *et al*, *Nucl. Phys.* **A405**, 381 (1982); **A407**, 221 (1983)
- [4] J X Wei *et al*, *Phys. Rev. Lett.* **67**, 3368 (1991)
- [5] C R Morton *et al*, *Phys. Rev. Lett.* **72**, 4074 (1994)
- [6] J R Leigh *et al*, *Phys. Rev.* **C52**, 3151 (1995)
- [7] A M Stefanini *et al*, *Phys. Rev. Lett.* **74**, 864 (1995)
- [8] J D Bierman *et al*, *Phys. Rev. Lett.* **76**, 1587 (1996); *Phys. Rev.* **C54**, 3068 (1996)
- [9] N Rowley *et al*, *Phys. Lett.* **B254**, 25 (1991)
- [10] N Rowley, *Proc. Int. Workshop on Rare Nuclear Processes, November 1998, New Delhi* (to be published) (1999)
- [11] A M Stefanini, *Proc. Int. Workshop on Rare nuclear Processes, November 1998, New Delhi* (to be published) (1999)
- [12] Lagy T Baby *et al*, *Int. Workshop on Rare Nuclear Processes, November 1998, New Delhi* p2
- [13] J M Nieminen *et al*, *Phys. Rev. Lett.* **78**, 3832 (1997)
- [14] D J Hinde *et al*, *Phys. Rev. Lett.* **74**, 1295 (1995)
- [15] P G Hansen *et al*, *Annu. Rev. Nucl. Part. Sci.* **45**, 591 (1995)
- [16] C H Dasso and R Donangelo, *Phys. Lett.* **B276**, 1 (1991)
- [17] N Takigawa and H Sagawa, *Phys. Lett.* **B265**, 23 (1991)

- [18] M S Hussein *et al*, *Phys. Rev.* **C46**, 377 (1992); *Phys. Rev. Lett.* **72**, 2693 (1994); *Nucl. Phys.* **A588**, 85c (1995)
- [19] C H Dasso *et al*, *Phys. Rev.* **C50**, R12 (1994); *Nucl. Phys.* **A597**, 473 (1996)
- [20] N Takigawa *et al*, *Phys. Rev.* **C47**, R2470 (1993)
- [21] C Signorini *et al*, *Eur. Phys. J.* **A2**, 227 (1998)
- [22] V Fekou–Youimbi *et al*, *Nucl. Phys.* **A583**, 811c (1995)
- [23] A Yoshida *et al*, *Phys. Lett.* **B389**, 457 (1996)
- [24] M Dasgupta *et al*, *Phys. Rev. Lett.* (In press)
- [25] R Bass, *Phys. Rev. Lett.* **39**, 265 (1977)
- [26] K Hagino *et al*, *Phys. Rev. Lett.* **79**, 2014 (1997)
- [27] J P Glickman *et al*, *Phys. Rev.* **C43**, 1740 (1991)
- [28] Minfang Yeh *et al*, *Phys. Rev. Lett.* **76**, 1208 (1996)
- [29] M Dasgupta *et al*, *J. Phys.* **G23**, 1491 (1997)
- [30] M J Martin, *Nucl. Data Sheets* **47**, 797 (1986)
- [31] J S Eck *et al*, *Phys. Rev.* **C27**, 1807 (1983)
- [32] J Takahashi *et al*, *Phys. Rev. Lett.* **78**, 30 (1997)
- [33] A Mukerjee and B Dasmahapatra, *Nucl. Phys.* **A614**, 238 (1997)
- [34] C Signorini, *J. Phys.* **G23**, 1235 (1997)